Kinematic Mapping Based Assembly Mode Evaluation of Spherical Four-Bar Mechanisms

Hans-Peter Schröcker Manfred Husty
Unit Geometry and CAD, Institut of Basic Sciences
in Civil Engineering, University Innsbruck

December 15, 2006

Abstract

This paper presents a geometric interpretation of spherical four-bar motions as intersection curve of two quadrics, similar to the case of planar four-bar motions. We give a geometric characterization of the quadrics and use it for determining if two task positions of a spherical four-bar linkage lie on separate assembly modes of a coupler curve, known as "assembly mode defect."

Keywords: spherical kinematic mapping, spherical four-bar, branch defect, assembly mode defect.

1. Introduction

An important problem in the five-position synthesis of spherical four-bar linkages is the separation of task positions due to a discontinuous coupler curve, which is termed "assembly mode defect": In order to reach the prescribed input orientations, the mechanism has to be disassembled and re-assembled in a different way. Mechanisms with this defect are unusable in practice. Therefore, methods for effective and early recognition of assembly mode defective solutions to the synthesis problem are of interest.

Given the mechanism dimensions and the crank angles of the prescribed orientations, it is always possible to decide whether the orientations fall within the same assembly mode or not. If the mechanism has two assembly modes, one can identify two disjoint sub-intervals I_1, $I_2 \subset (0, 2\pi)$ of the input crank angle (see Murray and Larochelle 1998). The mechanism is assembly mode defective, if the prescribed orientations belong to

crank angles in both intervals I_1 and I_2. However, this method is rather cumbersome: It requires knowing the mechanism dimensions as well as the input crank angles.

Recently, Brunnthaler et al. 2006 proposed an efficient kinematic-mapping based synthesis algorithm for spherical four-bars. It allows to compute in full generality, i.e., without specifying the orientation parameters, a univariate polynomial P of degree six that governs the solutions to the synthesis problem. Any pair of real roots of P can be combined to produce a spherical four-bar. Hence, the synthesis problem has up to 15 real solutions. They might, however, be afflicted with an assembly mode defect. In the paper at hand we present a simple kinematic mapping based assembly mode test. It can be combined with the algorithm of Brunnthaler et al. 2006 to provide a homogeneous design environment for five position synthesis of spherical four bars.

The assembly mode test we propose transforms the problem to the assembly mode test for planar four-bars of Schröcker et al. 2007. For computing the transformation, we make use of the fact that the spherical kinematic image of a four-bar motion is the intersection curve of two quadrics Q_1 and Q_2 (similar to the well-known fact for planar four-bar motions, see Bottema and Roth 1990, Chapter 12). For spherical four-bar motions this was recently observed in Brunnthaler et al. 2006 (implicitely it was already used in Bulca and Husty 1995). A detailed study of the geometry of the quadrics Q_i is a necessary prerequisite for our assembly mode test and a further contribution of the present article.

In Section 2 we recall basic notions and concepts of spherical kinematic mapping. Sections 3 and 4 are dedicated to an analytic description and a geometric characterization of the image curve of spherical four-bar motions. The actual assembly mode test is derived in Section 5. In Section 6 we present numerical examples.

2. Preliminaries

Spherical Euclidean displacements $\mathcal{D}$ can be described by

$$\mathbf{X} = \mathbf{A} \cdot \mathbf{x}, \tag{1}$$

where $\mathbf{X}$ and $\mathbf{x}$ represent a point in the fixed and moving frame, respectively, and $\mathbf{A} \in \mathrm{SO}(3)$ is a 3×3 proper orthogonal matrix (Husty et al. 1997; McCarthy 2000). For the following it is convenient to use the Euler parameterization of $\mathrm{SO}(3)$:

$$\mathbf{A} := \begin{bmatrix} x_0^2 + x_1^2 - x_2^2 - x_3^2 & 2(x_1x_2 - x_0x_3) & 2(x_1x_3 + x_0x_2) \\ 2(x_1x_2 + x_0x_3) & x_0^2 + x_2^2 - x_1^2 - x_3^2 & 2(x_2x_3 - x_0x_1) \\ 2(x_1x_3 - x_0x_2) & 2(x_0x_1 + x_2x_3) & x_0^2 + x_3^2 - x_1^2 - x_2^2 \end{bmatrix}. \tag{2}$$

In the matrix $\mathbf{A}$ the entries x_i have been normalized so that

$$x_0^2 + x_1^2 + x_2^2 + x_3^2 = 1. \tag{3}$$

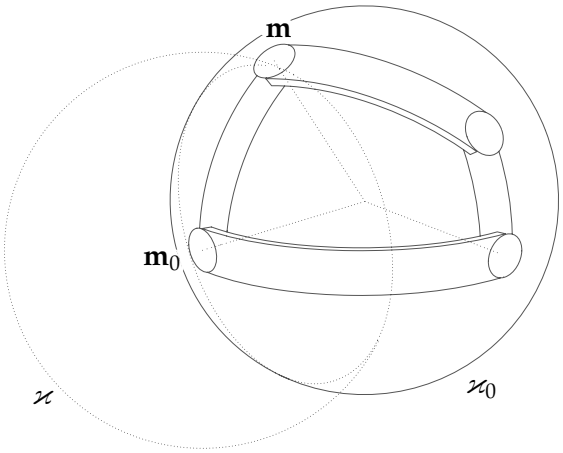

Figure 1: Spherical four-bar

We refer to Equation (3) as the *first normalizing condition*. The mapping

$$\begin{aligned} \varkappa\colon \mathcal{D} &\to \mathbf{p} \in P^3, \\ \mathbf{A} = \mathbf{A}(x_i) &\mapsto [x_0 : x_1 : x_2 : x_3]^T \neq [0:0:0:0]^T \end{aligned} \tag{4}$$

is called *spherical kinematic mapping* and maps each spherical Euclidean displacement $\mathcal{D}$ to a point $\mathbf{p}$ in P^3. The space P^3 is called kinematic image space and is naturally endowed with an elliptic metric (Blaschke 1960). Changes of coordinates in either the moving or fixed frame induce collineations of P^3 that fix the absolute quadric E of elliptic geometry (compare Section 4).

3. Kinematic image of spherical four-bars

In a spherical four-bar two points of the coupler revolute joint move on circles. In Figure 1 this is shown for the point $\mathbf{m}$. When we want to model this constraint we can say that point $\mathbf{m}$ is constrained to be on two spheres. One is the unit sphere $\varkappa_0$ the other is a sphere $\varkappa$ centered at the piercing point $\mathbf{m}_0$ of the base revolute joint with the unit sphere and radius $r = \overline{\mathbf{m}\mathbf{m}_0}$. Let the vector of the fixed revolute axis be $[A, B, C]^T$ and let the corresponding vector of the moving revolute axis in the coupler system be $[a, b, c]^T$. The endpoints of these vectors will be $\mathbf{m}_0$ resp. $\mathbf{m}$ when we have the side conditions

$$A^2 + B^2 + C^2 = 1, \quad \text{and} \quad a^2 + b^2 + c^2 = 1. \tag{5}$$

We refer to Equation (5) as the *second normalizing condition*. The path of $\mathbf{m}$ is now modeled as the intersection curve of the two spheres:

$$\varkappa_0\colon X_1^2 + X_2^2 + X_3^2 - X_0^2 = 0, \tag{6}$$

$$\varkappa\colon X_1^2 + X_2^2 + X_3^2 - 2AX_0X_1 - 2BX_0X_2 - 2CX_0X_3 + RX_0^2 = 0. \tag{7}$$

with $R = A^2 + B^2 + C^2 - r^2 = 1 - r^2$, where r is the radius of the sphere $\varkappa$ and A, B, C are the coordinates of the sphere center. Note that R is confined to the interval $(-3, 1)$ in order to ensure a real intersection of $\varkappa_0$ and $\varkappa$.

X_i are the coordinates of the moving pivot in the fixed system and can be computed via Equation (1). We substitute $[X_0, X_1, X_2, X_3]^T = \mathbf{A} \cdot [a, b, c]^T$ into Equation (7). Simplifying the result using Equation (6) (which is automatically met if the normalizing conditions (3) and (5) hold) and the first normalization condition (3) we obtain the constraint equation of a surface $Q \subset P^3$. Denoting by $\mathbf{E}$ the four by four unit matrix and letting $\mathbf{x} = [x_0, x_1, x_2, x_3]^T$, the equation of Q reads

$$Q\colon \mathbf{x}^T \cdot \mathbf{Q} \cdot \mathbf{x} = 0 \tag{8}$$

where

$$\mathbf{Q} = \mathbf{Q}^\star - \frac{1+R}{2} \cdot \mathbf{E}, \quad R \in (-3, 1), \tag{9}$$

and

$$\mathbf{Q}^\star = \begin{bmatrix} Aa + Bb + Cc & Cb - Bc & Ac - Ca & Ba - Ab \\ Cb - Bc & Aa - Bb - Cc & Ab + Ba & Ac + Ca \\ Ac - Ca & Ab + Ba & -Aa + Bb - Cc & Bc + Cb \\ Ba - Ab & Ac + Ca & Bc + Cb & -Aa - Bb + Cc \end{bmatrix}. \tag{10}$$

Q is a quadratic surface in P^3 and can be conveniently used for the analysis of spherical four-bar mechanisms following the process demonstrated in Bottema and Roth 1990 for planar four-bar mechanisms. The four-bar motion is mapped to the intersection curve of two quadrics of type (8)–(10) in the image space and can easily be investigated using the properties of the image space curve.

4. Geometric characterization

In this section we will give a geometric characterization of the quadric Q defined by Equations (8)–(10). We already mentioned that the geometry in P^3 is elliptic (Blaschke 1960); a change of coordinates in either the moving or the fixed system induces a projective transformation of P^3 that leaves fixed the *absolute quadric*

$$E\colon \mathbf{x}^T \cdot \mathbf{E} \cdot \mathbf{x} = 0. \tag{11}$$

Note that the quadric E contains no real points.

Theorem 1. *The quadrics Q defined by Equations* (8)–(10) *are precisely the quadrics with infinitely many real points whose intersection with E consists of two pairs of conjugate complex lines S, $\overline{S}$ and T, $\overline{T}$ that form a spatial quadrilateral (Figure 2).*

Before we give the proof of Theorem 1, we shortly discuss how to verify that a straight line L with Plücker coordinate vector $\mathbf{l} = [l_0 : \ldots : l_5]^T$ is contained in the quadric $Q\colon \mathbf{x}^T \cdot \mathbf{Q} \cdot \mathbf{x} = 0$. This will be needed during the proof of Theorem 1.

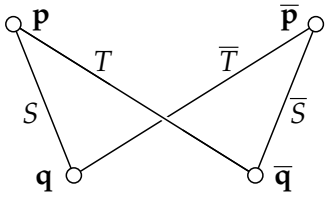

Figure 2: Intersection of E and Q

Generically, the intersection points of L and the coordinate planes $\zeta_i\colon x_i = 0$ can be computed by the formulas

$$\begin{aligned} L \cap \zeta_0 &= \mathbf{l}_0 = [\ \ 0 : \quad l_0 : \quad l_1 : \quad l_2]^T, \\ L \cap \zeta_1 &= \mathbf{l}_1 = [-l_0 : \quad 0 : \quad l_5 : -l_4]^T, \\ L \cap \zeta_2 &= \mathbf{l}_2 = [-l_1 : -l_5 : \quad 0 : \quad l_3]^T, \\ L \cap \zeta_3 &= \mathbf{l}_3 = [-l_2 : \quad l_4 : -l_3 : \quad 0]^T \end{aligned} \tag{12}$$

(Pottmann and Wallner 2001, Section 2.1). The formula for $\mathbf{l}_i$ fails (i.e., $\mathbf{l}_i$ is zero) iff $L \subset \zeta_i$. We conclude that at most two of the above formulas fail and at least two of the points $\mathbf{l}_0, \ldots, \mathbf{l}_3$ (say $\mathbf{l}_i$ and $\mathbf{l}_j$) are different. Now we consider the polynomial

$$P(t) = (\mathbf{l}_i + t\mathbf{l}_j)^T \cdot \mathbf{Q} \cdot (\mathbf{l}_i + t\mathbf{l}_j). \tag{13}$$

Generically, $P(t)$ is of degree two and its roots correspond to the intersection points of L and Q. *The straight line L is contained in Q if and only if* (13) *vanishes identically in t.*

Proof of Theorem 1. At first we show that any quadric Q of the shape (8)–(10) satisfies the characterizing conditions of the theorem. The restriction of R to the interval $(-3, 1)$ guarantees that Q contains infinitely many real points. Furthermore, the characteristic polynomial of the pencil of quadrics spanned by E and Q is

$$16 \det(\mathbf{Q} + \lambda \mathbf{E}) = (2\lambda + 1 - R)^2 (2\lambda - 3 - R)^2. \tag{14}$$

It has two roots of multiplicity two. From this we can already conclude that the intersection $Q \cap E$ consists of four straight lines (see Sommerville 1934, p. 268). Because Q and E can be described by real equations and E contains no real points, this set of lines consists of two pairs $(S, \overline{S})$ and $(T, \overline{T})$ of conjugate complex lines. These pairs of conjugate complex lines are necessarily skew because otherwise their intersection point would be real – a contradiction to the fact that E contains no real points. Furthermore, no three of the lines S, $\overline{S}$, T and $\overline{T}$ can be skew because otherwise E and Q would be equal. Hence elements of opposite pairs are intersecting and the lines S, $\overline{S}$, T, $\overline{T}$ form a spatial quadrilateral.

Assume now conversely that Q' is a quadric with infinitely many real points that intersects E in four straight lines S', $\overline{S}'$, T', $\overline{T}'$, as required by the theorem. We have

to show there exist values a, b, c, A, B, C and R such that Q' equals the quadric Q of (8)–(10).

The intersection lines of Q' and E can be written as

$$[\mathbf{s}', \mathbf{s}']^T, \quad [\overline{\mathbf{s}}', \overline{\mathbf{s}}']^T, \quad [\mathbf{t}', -\mathbf{t}']^T, \quad [\overline{\mathbf{t}}', -\overline{\mathbf{t}}']^T \tag{15}$$

where

$$\mathbf{s}' = \begin{bmatrix} 1+s^2 \\ 2s\mathrm{i} \\ (s^2-1)\mathrm{i} \end{bmatrix}, \quad \mathbf{t}' = \begin{bmatrix} 1+t^2 \\ 2t\mathrm{i} \\ (t^2-1)\mathrm{i} \end{bmatrix}, \quad s, t \in \mathbb{C} \cup \infty. \tag{16}$$

The intersection lines of Q and E can be written as

$$[\mathbf{s}, \mathbf{s}]^T, \quad [\overline{\mathbf{s}}, \overline{\mathbf{s}}]^T, \quad [\mathbf{t}, -\mathbf{t}]^T, \quad [\overline{\mathbf{t}}, -\overline{\mathbf{t}}]^T \tag{17}$$

where

$$\mathbf{s} = \begin{bmatrix} -AC - B\mathrm{i} \\ -BC + A\mathrm{i} \\ A^2 + B^2 \end{bmatrix}, \quad \mathbf{t} = \begin{bmatrix} -ac - b\mathrm{i} \\ -bc + a\mathrm{i} \\ a^2 + b^2 \end{bmatrix}. \tag{18}$$

Equations (15) to (18) can be verified using the procedure described right before this proof. We let

$$A := \frac{-2\Im(s)}{\Re(s)^2 + \Im(s)^2 + 1}, \quad B := \frac{\Re(s)^2 + \Im(s)^2 - 1}{\Re(s)^2 + \Im(s)^2 + 1}, \quad C := \frac{-2\Re(s)}{\Re(s)^2 + \Im(s)^2 + 1} \tag{19}$$

and

$$a := \frac{-2\Im(t)}{\Re(t)^2 + \Im(t)^2 + 1}, \quad b := \frac{\Re(t)^2 + \Im(t)^2 - 1}{\Re(t)^2 + \Im(t)^2 + 1}, \quad c := \frac{-2\Re(t)}{\Re(t)^2 + \Im(t)^2 + 1}. \tag{20}$$

These values are real and satisfy $a^2 + b^2 + c^2 = A^2 + B^2 + C^2 = 1$. Furthermore, substitution of (19) and (20) into (18) yields vectors $\mathbf{s}$, $\mathbf{t}$ that are proportional to $\mathbf{s}'$, $\mathbf{t}'$. Hence, we can build the quadric $Q^\star$ of Equation (10) using the values (19) and (20) for a, b, c and A, B, C. The intersection of $Q^\star$ and E (and hence also of Q and E) will consists of the straight lines $S' = S$, $\overline{S}' = \overline{S}$, $T' = T$ and $\overline{T}' = \overline{T}$. The quadric Q' lies in the pencil spanned by $Q^\star$ and E and there exists a value $R \in \mathbb{C}$ such that the quadric Q of (9) equals Q'. Because Q' contains infinitely many real points, R is real and contained in the interval $(-3, 1)$. This finishes the proof. □

Corollary 1. *The straight lines S and $\overline{S}$ depend only on A, B and C. The straight lines T and $\overline{T}$ depend only on a, b and c.*

Proof. The corollary follows from Equations (17) and (18), where the Plücker coordinates of S are given in terms of A, B, C and the Plücker coordinates of T are given in terms of a, b, c. □

Remark 1. The intersection of E and Q is independent of R. We can view R as the pencil parameter of the pencil of quadrics spanned by E and Q. In other words, varying R yields quadrics Q and $\tilde{Q}$ that intersect in four conjugate complex lines S, $\overline{S}$, T and $\overline{T}$. Hence Q and $\tilde{Q}$ have no real intersection points. This is similar to the kinematic image of planar four-bars where it has been exploited for workspace and tolerance analysis (see Husty 1996 and Hofmeister et al. 2006). The ideas of these articles could, in principle, also be used for the workspace and tolerance analysis of spherical mechanisms.

5. Assembly mode decisions for spherical four-bar mechanisms

The introductory comments on the necessity of efficient elimination of assembly mode defective solutions to synthesized four-bars not only apply to the spherical case but also to planar four-bar synthesis. As an accompanying tool to recent kinematic mapping based five-position synthesis algorithms for planar four-bar mechanisms (Brunnthaler et al. 2005; Hayes and Zsombor-Murray 2002) a simple kinematic mapping based test for deciding whether two positions of a planar four-bar lie within the same assembly mode or not has been presented in Schröcker et al. 2005 and Schröcker et al. 2007. It is based on the solution of two quadratic equations and, depending on the number of real roots, a subsequent interval determination or sign comparison. In Section 5.2 we will show that this algorithm can also be used for spherical assembly mode decisions. We summarize the algorithm for the planar case in the following section.

5.1 **Planar four-bar mechanisms.** Similar to the spherical case, the kinematic image of a planar four-bar is the intersection curve of two quadrics (hyperboloids) H_0 and H_1 in P^3. The equations of H_0 and H_1 are $H_i\colon \mathbf{x}^T \cdot \mathbf{H}_i \cdot \mathbf{x} = 0$ where $\mathbf{H}_i$ is of the shape

$$\mathbf{H} = \begin{bmatrix} (a-\xi)^2+(b-\eta)^2-\varrho^2 & 2\eta-2b & 2a-2\xi & 2b\xi-2a\eta \\ 2\eta-2b & 4 & 0 & -2a-2\xi \\ 2a-2\xi & 0 & 4 & -2b-2\eta \\ 2\xi b-2\eta a & -2a-\xi & -2b-\eta & (a+\xi)^2+(b+\eta)^2-\varrho^2 \end{bmatrix}, \quad (21)$$
$$\xi, \eta, a, b, \varrho \in \mathbb{R}.$$

The hyperboloid $H\colon \mathbf{x}^T \cdot \mathbf{H} \cdot \mathbf{x} = 0$ is the constraint surface of all proper Euclidean motions such that the image of the point $(\xi, \eta)^T$ lies on the circle with center $(a, b)^T$ and radius ϱ.

Lemma 1. *Any hyperboloid of the shape* (21) *can be characterized geometrically by the following two properties:*

1. *H contains the points $\mathbf{i} = [0:1:\mathrm{i}:0]^T$ and $\bar{\mathbf{i}} = [0:1:-\mathrm{i}:0]^T$.*
2. *H is tangent to the planes $\omega = [1:0:0:\mathrm{i}]$ and $\overline{\omega} = [1:0:0:-\mathrm{i}]$*

(see Figure 3).

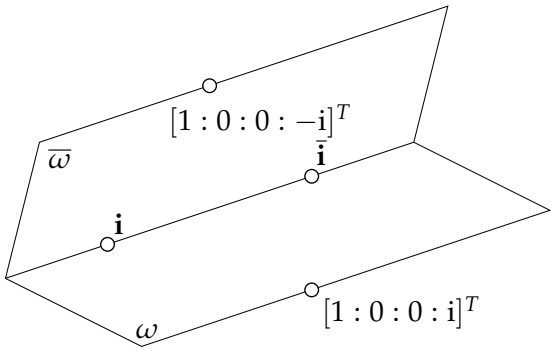

Figure 3: Geometric characterization of the quadric (21).

A proof of this lemma is given in Bottema and Roth 1990, Chapter 11.7.

Via planar kinematic mapping, the four-bar motion is identified with the intersection curve C of two hyperboloids H_0 and H_1 (if a kinematic mapping based synthesis algorithm is used, the hyperboloids H_0 and H_1 are readily available). The kinematic images of two prescribed positions are the precision points $\mathbf{p}$, $\mathbf{q} \in C$. Branch defect occurs if and only if, $\mathbf{p}$ and $\mathbf{q}$ lie in different branches of C. This can be tested by computing the roots z_i of the quadratic equations

$$\begin{aligned} T_1(z) &:= \|\mathbf{m}_1(z) - \mathbf{m}_2(z)\|^2 - (r_1(z) + r_2(z))^2 = 0, \\ T_2(z) &:= \|\mathbf{m}_1(z) - \mathbf{m}_2(z)\|^2 - (r_1(z) - r_2(z))^2 = 0, \end{aligned} \tag{22}$$

where

$$\mathbf{m}(z) = 1/2 \begin{pmatrix} b - \eta + z(a + \xi) \\ -a + \xi + z(b + \eta) \\ 2z \end{pmatrix} \tag{23}$$

and

$$r^2(z) = 1/4\, \varrho^2 (1 + z^2). \tag{24}$$

The zeros of (22) give the z-coordinate of points of C with horizontal tangents. Now three cases have to be distinguished:

Case 1: Two roots of (22) are real and two are conjugate complex. In this case the planar four-bar has only one assembly mode and nothing more needs to be done.

Case 2: Equation (22) has four real roots z_0, z_1, z_2 and z_3. In this case we consider the z-coordinates z_p and z_q of $\mathbf{p}$ and $\mathbf{q}$. The points $\mathbf{p}$ and $\mathbf{q}$ lie in the same branch of C if and only if the interval $[z_p, z_q]$ contains either none or all of the values z_i.

Case 3: Equation (22) has four complex roots. In this case, we consider the quantities

$$\Delta_p = \det\big(\mathbf{m}_1'(z_p) - \mathbf{p}', \mathbf{m}_2'(z_p) - \mathbf{p}'\big) \quad \text{and} \quad \Delta_q = \det\big(\mathbf{m}_1'(z_q) - \mathbf{q}', \mathbf{m}_2'(z_q) - \mathbf{q}'\big) \tag{25}$$

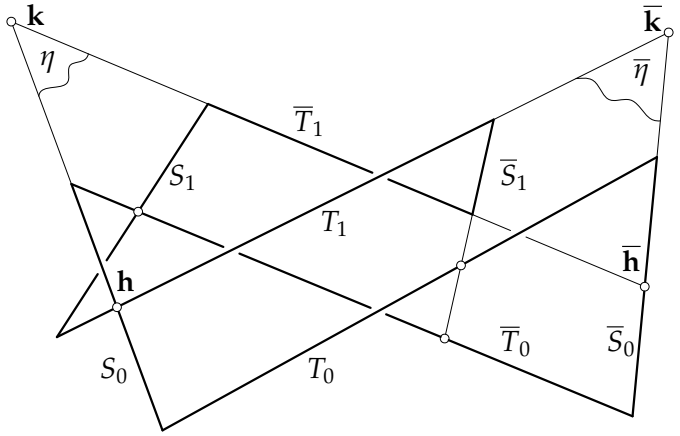

Figure 4: Configuration of the eight lines S_i, $\overline{S}_i$ T_i, $\overline{T}_i$ $(i = 0, 1)$

(prime denotes projection onto the plane $z = 0$, i.e., dropping of the z-coordinate). The points $\mathbf{p}$ and $\mathbf{q}$ lie in the same branch of C if and only if Δ_p and Δ_q are of the same sign.

Detailed proofs of the correctness of this assembly mode test are given in Schröcker et al. 2005 and Schröcker et al. 2007.

5.2 **Spherical four-bar mechanisms.** In principle, the situation in spherical kinematics is the same as in planar kinematics, except that we have to use quadrics Q_0, Q_1 of shape (8)–(10) instead of H_0 and H_1. Given the kinematic images $\mathbf{p}$ and $\mathbf{q}$ of two orientations of the spherical four-bar, we have to decide whether $\mathbf{p}$ and $\mathbf{q}$ lie in different branches of $C := Q_0 \cap Q_1$ or not. This question is of topological nature. In particular, it is invariant with respect to real projective transformations. In the following we will show that there exists a *regular real projective transformation* $\alpha\colon P^3 \to P^3$ that maps the two quadrics Q_i onto two quadrics H_i of the shape (21). Performing the assembly mode test of Section 5.1 with $H_0 = \alpha(Q_0)$, $H_1 = \alpha(Q_1)$, $\alpha(\mathbf{p})$ and $\alpha(\mathbf{q})$ as input data will tell whether the orientations to $\mathbf{p}$ and $\mathbf{q}$ lie in the same assembly mode of the spherical four-bar or not.

Theorem 2. *To any two quadrics Q_0, Q_1 of the shape* (8)–(10) *there exists a real projective transformations $\alpha\colon P^3 \to P^3$ that transforms Q_0 and Q_1 into quadrics H_0, H_1 of the shape* (21).

Proof. We give a constructive proof that exploits the geometric properties of the hyperboloids H_i and the quadrics Q_i. The complete intersection of Q_i and E consists of four straight lines S_i, $\overline{S}_i$, T_i and $\overline{T}_i$ $(i = 0, 1$; see Figure 4). Because these lines are generators of E, the lines S_0 and T_1 are intersecting. They intersect in a point $\mathbf{h} = S_0 \cap T_1$ and span a plane $\eta = S_0 \vee \overline{T}_1$. Since S_0 and $\overline{T}_1$ are intersecting as well, we have

$$\mathbf{h} \in \eta, \quad \overline{\mathbf{h}} \in \eta, \quad \mathbf{h} \in \overline{\eta}, \quad \overline{\mathbf{h}} \in \overline{\eta}. \tag{26}$$

A homogeneous coordinate vector of $\mathbf{h}$ is

$$\begin{bmatrix} (1-C_0^2)(1-c_1^2)-(1-c_1C_0)(b_1B_0+a_1A_0) \\ (1-c_1^2)B_0C_0-(1-C_0^2)b_1c_1 \\ -(1-c_1^2)A_0C_0+(1-C_0^2)a_1c_1 \\ (B_0a_1-A_0b_1)(C_0c_1-1) \end{bmatrix} + \mathrm{i}\cdot \begin{bmatrix} (c_1-C_0)(B_0a_1-A_0b_1) \\ a_1(1-C_0^2)-A_0(1-c_1^2) \\ b_1(1-C_0^2)-B_0(1-c_1^2) \\ (C_0-c_1)(A_0a_1+B_0b_1) \end{bmatrix}; \quad (27)$$

a homogeneous coordinate vector of η is

$$\begin{bmatrix} -(1+c_1C_0)(A_0a_1+B_0b_1)-(1-C_0^2)(1-c_1^2) \\ -B_0C_0(1-c_1^2)+b_1c_1(1-C_0^2) \\ A_0C_0(1-c_1^2)-a_1c_1(1-C_0^2) \\ (1+c_1C_0)(A_0b_1-B_0a_1) \end{bmatrix} + \mathrm{i}\cdot \begin{bmatrix} (c_1+C_0)(A_0b_1-B_0a_1) \\ A_0(1-c_1^2)+a_1(1-C_0^2) \\ B_0(1-c_1^2)+b_1(1-C_0^2) \\ (c_1+C_0)(A_0a_1+B_0b_1) \end{bmatrix}. \quad (28)$$

We denote by $\Re(\mathbf{h})$, $\Im(\mathbf{h})$, $\Re(\eta)$ and $\Im(\eta)$ the respective real and imaginary parts of (27) and (28). It is easy to see that (26) is equivalent to

$$\Re(\eta)^T\Re(\mathbf{h}) = \Re(\eta)^T\Im(\mathbf{h}) = \Im(\eta)^T\Re(\mathbf{h}) = \Im(\eta)^T\Im(\mathbf{h}) = 0. \quad (29)$$

In other words: *Real and imaginary part of* $\mathbf{h}$ *lie in real and imaginary part of* η. There exists a real projective transformation α that maps $\Re(\mathbf{h})$ to $[1,0,0,0]^T$, $\Im(\mathbf{h})$ to $[0,0,0,1]^T$ and arbitrary real points of $\Re(\eta)$ and $\Im(\eta)$ to $[0,1,0,0]^T$ and $[0,0,1,0]^T$, respectively (in fact, there exists an infinity of such transformations). Because the defining conditions on α are real, we can assume that α itself is real. This implies

$$\alpha(\mathbf{h}) = \mathbf{i}, \quad \alpha(\overline{\mathbf{h}}) = \overline{\mathbf{i}}, \quad \alpha(\eta) = \omega, \quad \alpha(\overline{\eta}) = \overline{\omega}. \quad (30)$$

Hence, the α-images of Q_i satisfy the geometric characterization of the hyperboloids H_i which finishes the proof. □

5.2.1 *The transformation formula.* The proof of Theorem 2 is constructive but actual formulas for α are missing. We will derive them in the following. The projective transformation α maps a point $\mathbf{x}$ to $\alpha(\mathbf{x}) = \mathbf{A}\cdot\mathbf{x}$ where $\mathbf{A}$ is a real, regular four by four matrix. We will compute $\mathbf{A}^{-1}$ instead of $\mathbf{A}$. Because we may assume

$$\mathbf{A}\cdot\Re(\mathbf{h}) = [0:1:0:0]^T \quad \text{and} \quad \mathbf{A}\cdot\Im(\mathbf{h}) = [0:0:1:0]^T, \quad (31)$$

the second and third column of $\mathbf{A}^{-1}$ can be taken as $\Re(\mathbf{h})$ and $\Im(\mathbf{h})$, respectively. The first and fourth column can be taken as real and imaginary part of any point in η. A simple choice is $\mathbf{k} := S_0 \cap \overline{T}_1$ whose real and imaginary part equal $\Re(\eta)$ and $\Im(\eta)$ (because η is tangent to E in $\mathbf{k}$ and the polar system of E is described by the identity matrix). Hence, the matrix $\mathbf{A}^{-1}$ can be written as

$$\mathbf{A}^{-1} = [\Re(\eta), \Re(\mathbf{h}), \Im(\mathbf{h}), \Im(\eta)]. \quad (32)$$

Equation (32) describes the transformation α^{-1} directly in terms of parameters of the spherical four-bar mechanism. This inverse transformation is needed for computing the equation of $H_i = \alpha(Q_i)$. It is $H_i\colon \mathbf{x}^T \cdot \mathbf{H}_i \cdot \mathbf{x} = 0$ where

$$\mathbf{H}_i = (\mathbf{A}^{-1})^T \cdot \mathbf{Q}_i \cdot \mathbf{A}^{-1}. \tag{33}$$

Remark 2. The singularities of the suggested construction manifest in the vanishing of the determinant of $\mathbf{A}^{-1}$:

$$\begin{aligned}\det \mathbf{A}^{-1} = 4(A_0^2 + B_0^2)^2(a_1^2 + b_1^2)^2(a_1^2(B_0^2 + C_0^2) + b_1^2(A_0^2 + C_0^2) + c_1^2(A_0^2 + B_0^2) \\ - 2(A_0B_0a_1b_1 + A_0C_0a_1c_1 + B_0C_0b_1c_1)).\end{aligned} \tag{34}$$

This case is characterized by the failure of the span and intersection formulas for Plücker coordinates that we used to compute (27) and (28) (see Pottmann and Wallner 2001, Section 2.1). Because this failure has no geometric meaning, it is always possible to use our formulas after a suitable change of coordinates in the fixed and/or moving system.

5.2.2 *The assembly mode test.* The algorithm for making assembly mode decisions for spherical four-bars is as follows:

Step 1: From the mechanism dimensions compute the parameters a_i, b_i, c_i, A_i, B_i, C_i and R_i that describe the quadric Q_i via Equations (8)–(10).

Step 2: Compute the transformation α^{-1} according to Equation (32) and the transformation α.

Step 3: Compute the equations of hyperboloids H_i via Equation (33).

Step 4: Compute the planar precision points $\mathbf{q}_j$ from the spherical precision points $\mathbf{p}_j$ according to $\mathbf{q}_j = \alpha(\mathbf{p}_j)$.

Step 5: Make an assembly mode decision for the planar four-bar motion to $H_0 \cap H_1$ and the precision points $\mathbf{q}_j$. The spherical four-bar is afflicted with an assembly mode defect if and only if the planar four-bar is.

Remark 3. The hyperboloids H_0 and H_1 described by (33) are not in the general form of Equation (21). In fact, their entries h^i_{jk} satisfy the additional relations

$$h^0_{03} = 0,\ h^0_{02} = -h^0_{13},\ h^0_{01} = h^0_{23} \quad \text{and} \quad h^1_{03} = 0,\ h^1_{02} = h^1_{13},\ h^1_{01} = -h^1_{23} \tag{35}$$

plus the relations obtained from symmetry of $\mathbf{H}_i$. This implies that the base points of the corresponding four-bars are

$$(a_0, b_0)^T, \quad (0,0)^T \tag{36}$$

(i.e., $a_1 = b_1 = 0$) while the coordinates of the coupler joint in the moving frame are

$$(0,0)^T, \quad (\xi_1, \eta_1)^T \tag{37}$$

(i.e., $\xi_0 = \eta_0 = 0$). This is no restriction of generality and can always be attained by choosing the coordinate frames in the fixed and moving frame appropriately.

Remark 4. The transformation (33) is independent of R. Hence it not only transforms two quadrics Q_0 and Q_1 to hyperboloids H_0 and H_1 but the complete pencil spanned by Q_i and E to a pencil of hyperboloids, spanned by H_i and $\alpha(E)$.

6. An Example

In this section we illustrate our algorithm with a comprehensive example. We consider the five position synthesis problem to the prescribed precision points

$$\begin{aligned}
&\mathbf{p}_0 = [1.0000 : 0.0000 : 0.0000 : 0.0000]^T, \qquad \mathbf{p}_1 = [1.0000 : 0.1875 : 1.7188 : 2.1875]^T,\\
&\mathbf{p}_2 = [1.0000 : 2.6207 : 0.3103 : 0.3793]^T, \qquad \mathbf{p}_3 = [1.0000 : 1.8333 : 0.6000 : 0.4333]^T,\\
&\mathbf{p}_4 = [1.0000 : 0.2969 : 0.6406 : 1.4844]^T.
\end{aligned} \tag{38}$$

Using the algorithm of Brunnthaler et al. 2006 we find that the synthesis problem has 15 real solutions. In kinematic image space they belong to the intersection curves $C_{ij} = Q_i \cap Q_j$ of the quadrics $Q_i \colon \mathbf{x}^T \cdot \mathbf{Q}_i \cdot \mathbf{x} = 0$ where

$$\begin{aligned}
\mathbf{Q}_0 &= \begin{bmatrix} -0.7768 & 0.4900 & -0.8305 & 0.0569 \\ 0.4900 & -0.9556 & -0.4523 & -0.6031 \\ -0.8305 & -0.4523 & -0.5480 & -0.3238 \\ 0.0569 & -0.6031 & -0.3238 & 0.2089 \end{bmatrix},\\
\mathbf{Q}_1 &= \begin{bmatrix} -0.6693 & 0.5430 & -0.7364 & -0.3364 \\ 0.5430 & -1.0021 & -0.6210 & 0.1019 \\ -0.7364 & -0.6210 & -0.5729 & -0.2367 \\ -0.3364 & 0.1019 & -0.2367 & 0.4596 \end{bmatrix},\\
\mathbf{Q}_2 &= \begin{bmatrix} -0.8339 & -0.9219 & -0.0939 & -0.2529 \\ -0.9219 & -0.2602 & 0.2063 & -0.1414 \\ -0.0939 & 0.2063 & -1.4807 & -0.3055 \\ -0.2529 & -0.1414 & -0.3055 & 0.3511 \end{bmatrix},\\
\mathbf{Q}_3 &= \begin{bmatrix} -0.3963 & 0.1389 & -0.9479 & -0.2543 \\ 0.1389 & -0.6534 & -0.3064 & 0.8575 \\ -0.9479 & -0.3064 & 0.1882 & 0.0417 \\ -0.2543 & 0.8575 & 0.0417 & 0.1811 \end{bmatrix},\\
\mathbf{Q}_4 &= \begin{bmatrix} -1.0532 & -0.8754 & 0.3249 & -0.0697 \\ -0.8754 & -0.4463 & -0.3133 & -0.2646 \\ 0.3249 & -0.3133 & -1.3313 & -0.6328 \\ -0.0697 & -0.2646 & -0.6328 & 0.0222 \end{bmatrix},\\
\mathbf{Q}_5 &= \begin{bmatrix} 1.1249 & 0.7027 & 0.0386 & -0.6034 \\ 0.7027 & 0.6108 & 0.6228 & 0.3145 \\ 0.0386 & 0.6228 & 0.4760 & 0.7318 \\ -0.6034 & 0.3145 & 0.7318 & 0.7880 \end{bmatrix}.
\end{aligned} \tag{39}$$

i	a_i	b_i	c_i	A_i	B_i	C_i	r_i^2
0	0.4164	0.3043	0.8568	−0.8366	−0.4749	0.2730	3.0357
1	0.7460	0.2726	0.6076	−0.5221	−0.6417	0.5618	2.8924
2	−0.0344	−0.8894	0.4558	−0.2582	0.6762	0.6900	3.1119
3	0.9805	0.0981	0.1701	−0.2658	−0.2859	0.9206	2.5284
4	−0.3547	−0.9076	0.2246	0.1342	0.5400	0.8309	3.4043
5	0.1817	0.9450	0.2721	0.6488	0.0535	0.7591	0.5001

Table 1: Solutions to the synthesis problem

The corresponding solutions for the parameters a_i, b_i, c_i A_i, B_i, C_i and r_i^2 are given in Table 1.

We will not discuss all 15 solutions but consider particular examples.

Example 1. We start with $C_{01} = Q_0 \cap Q_1$. The transformation matrix $\mathbf{A}^{-1}$ reads

$$\mathbf{A}^{-1} = \begin{bmatrix} 0.2165 & 0.8904 & -0.0310 & 0.0816 \\ 0.1726 & -0.1726 & 0.8947 & 0.1194 \\ -0.4139 & 0.4139 & 0.4053 & -0.0348 \\ 0.1081 & 0.0773 & 0.1851 & -0.4874 \end{bmatrix} \tag{40}$$

and the transformed quadric equations are $H_i\colon \mathbf{x}^T \cdot \mathbf{H}_i \cdot \mathbf{x} = 0$ where the matrices

$$\begin{aligned} \mathbf{H}_0 &= \begin{bmatrix} -0.2874 & -0.5696 & -0.0934 & 0.0000 \\ -0.5696 & 4.0000 & 0.0000 & 0.0934 \\ -0.0934 & 0.0000 & 4.0000 & -0.5696 \\ 0.0000 & 0.0934 & -0.5696 & -0.2874 \end{bmatrix}, \\ \mathbf{H}_1 &= \begin{bmatrix} -0.3475 & -0.4209 & -0.5317 & 0.0000 \\ -0.4209 & 4.0000 & -0.0000 & -0.5317 \\ -0.5317 & 0.0000 & 4.0000 & 0.4209 \\ 0.0000 & -0.5317 & 0.4209 & -0.3475 \end{bmatrix}. \end{aligned} \tag{41}$$

are computed according to (33). The circle tangent conditions (22) read

$$-0.0178 - 0.0658z - 0.0497z^2 = 0, \quad 0.0054 - 0.0658z - 0.0265z^2 = 0. \tag{42}$$

They have the four real roots

$$\zeta_0 = -0.9428, \quad \zeta_1 = -0.3805, \quad \zeta_2 = -2.5661, \quad \zeta_3 = 0.0798. \tag{43}$$

The transformed precision points $\mathbf{q}_i = \mathbf{A} \cdot \mathbf{p}_i$ are

$$\begin{aligned} &\mathbf{q}_0 = [0.4248 : 0.4538 : -0.0158 : 0.1602]^T, \quad \mathbf{q}_1 = [-0.1420 : 0.2835 : 0.2019 : -0.6417]^T, \\ &\mathbf{q}_2 = [0.3309 : 0.0880 : 0.3709 : 0.1132]^T, \quad \mathbf{q}_3 = [0.1951 : 0.1308 : 0.2955 : 0.0404]^T, \\ &\mathbf{q}_4 = [0.2048 : 0.3976 : 0.2508 : -0.7895]^T. \end{aligned} \tag{44}$$

Their z-coordinates are

$$z_0 = 0.3772, \quad z_1 = 4.5198, \quad z_2 = 0.3422, \quad z_3 = 0.2068, \quad z_4 = -3.8556. \tag{45}$$

Any two of them enclose an interval $[z_i, z_j]$ that contains either all of the values ζ_i of (43) or none of them. Hence, all prescribed precision points can be reached within the same assembly mode.

Example 2. Next we turn our attention to the spherical four-bar to $C_{02} = Q_0 \cap Q_2$. In this case, the transformation matrix $\mathbf{A}^{-1}$ reads

$$\mathbf{A}^{-1} = \begin{bmatrix} -0.8161 & 0.2225 & -0.0875 & 0.3490 \\ -0.1793 & 0.1793 & 0.4151 & -0.4570 \\ -0.1095 & 0.1095 & -0.2940 & -0.7890 \\ 0.5384 & 0.4192 & -0.0543 & 0.2164 \end{bmatrix}. \tag{46}$$

The transformed matrices $\mathbf{H}_i$ are

$$\begin{aligned} \mathbf{H}_0 &= \begin{bmatrix} 9.8241 & -5.1622 & 11.1590 & 0.0000 \\ -5.1622 & 4.0000 & 0.0000 & -11.1590 \\ 11.1590 & 0.0000 & 4.0000 & -5.1622 \\ 0.0000 & -11.1590 & -5.1622 & 9.8241 \end{bmatrix}, \\ \mathbf{H}_1 &= \begin{bmatrix} 10.9828 & -11.1572 & -4.4625 & 0.0000 \\ -11.1572 & 4.0000 & 0.0000 & -4.4625 \\ -4.4625 & 0.0000 & 4.0000 & 11.1572 \\ 0.0000 & -4.4625 & 11.1572 & 10.9828 \end{bmatrix}. \end{aligned} \tag{47}$$

The circle tangent conditions (22) are

$$-25.5175 + 18.6785z - 69.0877z^2 = 0, \quad 37.9668 + 18.6785z - 5.6034z^2 = 0. \tag{48}$$

They have two real and two conjugate complex roots:

$$\zeta_0 = -1.4242, \quad \zeta_1 = 4.7576, \quad \zeta_{23} = 0.1352 \pm 0.5925\mathrm{i}. \tag{49}$$

We conclude that the spherical four-bar to C_{02} has only one assembly mode.

Example 3. Finally we make an assembly mode decision for the spherical four bar to C_{04}. The transformation matrix $\mathbf{A}^{-1}$ reads

$$\mathbf{A}^{-1} = \begin{bmatrix} -0.9312 & 0.1103 & 0.0161 & 0.1658 \\ -0.0370 & 0.0370 & 0.2629 & -0.6331 \\ -0.0807 & 0.0807 & -0.2194 & -0.7280 \\ 0.3536 & 0.3128 & 0.0199 & 0.2043 \end{bmatrix}. \tag{50}$$

The transformed matrices $\mathbf{H}_i$ are

$$\mathbf{H}_0 = \begin{bmatrix} 88.7583 & -17.1901 & 35.6379 & 0.0000 \\ -17.1901 & 4.0000 & 0.0000 & -35.6379 \\ 35.6379 & 0.0000 & 4.0000 & -17.1901 \\ 0.0000 & -35.6379 & -17.1901 & 88.7583 \end{bmatrix},$$
$$\mathbf{H}_1 = \begin{bmatrix} 51.1175 & -8.6796 & -18.6643 & 0.0000 \\ -8.6796 & 4.0000 & 0.0000 & -18.6643 \\ -18.6643 & 0.0000 & 4.0000 & 8.6796 \\ 0.0000 & -18.6643 & 8.6796 & 51.1175 \end{bmatrix}. \tag{51}$$

The circle tangent conditions (22)

$$-0.0304 + 0.0368z - 0.2155z^2 = 0, \quad 0.1967 + 0.0368z + 0.0116z^2 = 0 \tag{52}$$

have four complex roots

$$0.0854 \pm 0.3657\mathrm{i}, \quad -1.5918 \pm 3.8036\mathrm{i}. \tag{53}$$

The normal projections of the transformed points $\mathbf{q}_i = \mathbf{A} \cdot \mathbf{p}_i$ onto the plane $z = 0$ are

$$\begin{aligned} \mathbf{q}'_0 &= (-1.0051, -0.1469)^T, & \mathbf{q}'_1 &= (-26.3018, 7.5027)^T, \\ \mathbf{q}'_2 &= (-3.2393, -5.9493)^T, & \mathbf{q}'_3 &= (-3.4353, -3.5582)^T, \\ \mathbf{q}'_4 &= (-11.5293, 0.3056)^T. \end{aligned} \tag{54}$$

The normal projections of the centers $\mathbf{m}_{ij}(z_j)$ obtained by intersecting H_i with a horizontal plane through $\mathbf{q}_j$ are

$$\begin{aligned} \mathbf{m}'_{00} &= (-3.1734, -17.8189)^T, & \mathbf{m}'_{01} &= (44.4989, -17.8189)^T, \\ \mathbf{m}'_{02} &= (31.8348, -17.8189)^T, & \mathbf{m}'_{03} &= (26.7671, -17.8189)^T, \\ \mathbf{m}'_{04} &= (7.0413, -17.8189)^T \end{aligned} \tag{55}$$

and

$$\begin{aligned} \mathbf{m}'_{10} &= (7.0177, -4.3398)^T, & \mathbf{m}'_{11} &= (31.9847, -4.3398)^T, \\ \mathbf{m}'_{12} &= (25.3522, -4.3398)^T, & \mathbf{m}'_{13} &= (22.6982, -4.3398)^T, \\ \mathbf{m}'_{14} &= (12.3673, -4.3398)^T. \end{aligned} \tag{56}$$

The determinants $\Delta_j = \det(\mathbf{m}'_{0j} - \mathbf{q}'_j, \mathbf{m}'_{1j} - \mathbf{q}'_j)$ have values

$$\Delta_0 = 150.8697,\ \Delta_1 = 637.4517,\ \Delta_2 = 395.8222,\ \Delta_3 = 349.0752,\ \Delta_4 = 346.8475 \tag{57}$$

and are all of the same sign. From this we conclude that the synthesized four-bar is not assembly mode defective.

An overview of the number of real roots of the circle tangent conditions and assembly mode defects for all solution four-bars is given in Table 2. It is remarkable that none of the 15 real solutions suffers from an assembly mode defect.

ij	01	02	03	04	05	12	13	14	15	23	24	25	34	35	45
no. real roots	4	2	2	0	2	2	2	2	2	2	2	2	0	2	4
ass. mode def.	no	no	no	no	no	no	no	no	no	no	no	no	no	no	no

Table 2: Complete discussion of assembly mode defects.

7. Conclusion

We showed that the kinematic image of a spherical four-bar motion is the intersection curve of two quadrics Q_0 and $Q_1 \subset P^3$. The quadrics Q_i are characterized by the fact that their intersection with the quadric $E\colon\ x_0^2 + x_1^2 + x_2^2 + x_3^2 = 0$ is a spatial quadrilateral, formed by two pairs of conjugate complex lines.

We used this geometric characterization for an explicit description of a real projective transformation $\alpha\colon\ P^3 \to P^3$ that transforms Q_0 and Q_1 to two hyperboloids H_0 and H_1, respectively, whose intersection is the kinematic image of a planar four-bar motion and we demonstrated how to use the transformation α for assembly mode decisions of spherical four-bars.

References

Blaschke, W. (1960). *Kinematik und Quaternionen*. Mathematische Monographien. Springer.

Bottema, O. and B. Roth (1990). *Theoretical Kinematics*. Dover Publications.

Brunnthaler, K., M. Pfurner, and M. L. Husty (2005). Synthesis of planar four-bar mechanisms. In *Proceedings of MUSME 2005*, Uberlândia, Brazil.

Brunnthaler, K., H.-P. Schröcker, and M. L. Husty (2006). Synthesis of spherical four-bar mechanisms using spherical kinematic mapping. Accepted for publication in ARK 2006.

Bulca, F. and M. L. Husty (1995). Kinematic mapping of spherical three-legged platforms. In *Proceedings of the 15th Canada Congress of Applied Mechanics (CANCAM 1995)*, pp. 874–875.

Hayes, M. J. D. and P. J. Zsombor-Murray (2002). Solving the Burmester problem using kinematic mapping. In *Proceedings of DECT'02*, Montreal, Canada. ASME.

Hofmeister, A., W. Sextro, and O. Röschel (2006). Error workspace analysis of planar mechanisms. In M. Husty and H.-P. Schröcker (Eds.), *Proceedings of* EuCoMeS, *the first European Conference on Mechanism Science*, Obergurgl (Austria). Innsbruck University Press.

Husty, M., A. Karger, H. Sachs, and W. Steinhilper (1997). *Kinematik und Robotik*. Berlin, Heidelberg, New York: Springer.

Husty, M. L. (1996). On the workspace of planar three-legged platforms. In *Proc. World Automation Conf., 6th Int. Symposium on Rob. and Manuf. (ISRAM 1996)*, Volume 3, Montpellier (France), pp. 339–344.

McCarthy, J. M. (2000). *Geometric Design of Linkages*, Volume 320 of *Interdisciplinary Applied Mathematics*. New York: Springer.

Murray, A. P. and P. M. Larochelle (1998, September). A classification scheme for planar 4R, spherical 4R, and spatial RCCC linkages to facilitate computer animation. In *Proceedings of the 1998 ASME Design Engineering Technical Conferences*, Atlanta, Georgia. ASME Press.

Pottmann, H. and J. Wallner (2001). *Computational Line Geometry*. Springer.

Schröcker, H.-P., M. Husty, and J. M. McCarthy (2005). Kinematic mapping based evaluation of assembly modes for spherical four-bar synthesis. In *Proceedings of ASME 2005 29th Mechanism and Robotics Conference*, Long Beach.

Schröcker, H.-P., M. L. Husty, and J. M. McCarthy (2007). Kinematic mapping based assembly mode evaluation of planar four-bar mechanisms. Accepted for publication in Journal of Mechanical Design.

Sommerville, D. M. Y. (1934). *Analytical Geometry of Three Dimensions*. London: Cambridge University Press.